JACS
JOURNAL OF THE AMERICAN CHEMICAL SOCIETY
Article
pubs.acs.org/JACS

Guided Self-Assembly of Metal Atoms on Silicon Using Organic-Molecule Templating

Daniel R. Belcher,[†] Marian W. Radny,*[,†,‡] Steven R. Schofield,[§,∥] Phillip V. Smith,[†] and Oliver Warschkow[⊥]

[†]School of Mathematical and Physical Sciences, The University of Newcastle, Callaghan 2308, Australia
[‡]Institute of Physics, Poznan University of Technology, Poznan, Poland
[§]London Centre for Nanotechnology, University College London, London, WC1H 0AH, United Kingdom
[∥]Department of Physics and Astronomy, University College London, London, WC1E 6BT, United Kingdom
[⊥]Centre for Quantum Computation and Communication Technology, School of Physics, The University of Sydney, Sydney, NSW 2006, Australia

ABSTRACT: Assembling molecular components into low-dimensional structures offers new opportunities for nanoscale device applications. Here we describe the self-assembly of indium atoms into metallic chains on the silicon (001) surface using adsorbed benzonitrile molecules as nucleation and termination sites. Critically, individual benzonitrile adsorbates can be manipulated using scanning tunneling microscopy. This affords control over the position and orientation of the molecular adsorbates, which in turn determine the origin, direction, and length of the self-assembled metallic chains.

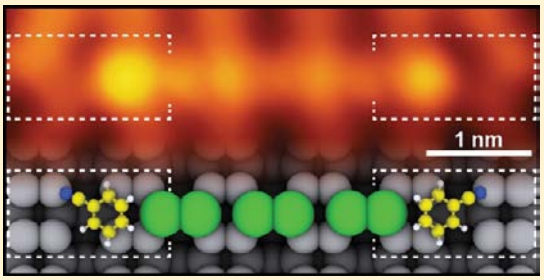

INTRODUCTION

The combination of organic and inorganic materials into low-dimensional structures on the Si(001) surface offers new possibilities for the development of nanoscale devices.[1] The self-assembly of organic molecules into one-dimensional structures is well established for the hydrogenated Si(001) surface.[2,3] Reactive dangling bonds serve as nucleation sites to which suitable organic molecules bind and assemble into one-dimensional chains. This process is controllable because the initial nucleation point can be created using an STM tip.[4] Inorganic structures are also known to self-assemble into one-dimensional structures on the bare Si(001) surface. This includes elemental adsorbates such as indium,[5−7] lead,[8] bismuth,[9] and rare earth metals,[10] which form atomic chains that run perpendicular to the dimer rows. These structures are often nucleated from surface defects and step edges, which are known to influence the reactivity of the surrounding dimers. For example, indium is mobile on the clean Si(001) surface at room temperature but becomes trapped[5,6] at C-defect sites, a common, water-related[11,12] surface feature that is chemically active. Attachment of a pair of indium atoms at a C-defect site modifies the surface such that a new chemically active site is produced on the adjacent row.[6] This produces a site of attachment for a second pair of indium atoms, and in this way indium atoms self-assemble into atomic chains on the surface. However, this type of chain growth is not particularly useful for nanoscale construction because C defects are randomly distributed on the surface[12] and cannot be repositioned or reoriented. As a result, no control exists over the position and length of the self-assembled atom chains.

We show here that control can be obtained over the growth of indium chains on Si(001) using an alternative molecular adsorbate that can be manipulated using an STM tip and yet mimics a C defect's ability to initiate chain growth. Such an adsorbate provides a means to predefine the position and length of the self-assembled indium atom chains. Our STM imaging and manipulation experiments demonstrate that benzonitrile (C_6H_5CN) satisfies these criteria and can thus be used as an organic template for inorganic nanoline growth.

METHODS

STM measurements were performed at room temperature under ultrahigh vacuum (<5 × 10^{-11} mbar) using an Omicron VT-STM. Substrates were cleaved from ⟨001⟩ orientated, n-type silicon wafers (0.08−0.1 Ω cm^{-1} antimony doped; Virginia Semiconductor Inc.), loaded into the UHV chamber, and prepared for use in experiments by degassing at ∼550 °C for 18 h. Atomically clean Si(001) surfaces were prepared by flash annealing the substrate to ∼1200 °C at the start of each experiment and then allowed to cool to room temperature before use. Benzonitrile (>99%; Sigma-Aldrich) was attached to the UHV chamber, with a separate pumping line to a turbo molecular pump used for purification, and admitted to the chamber via a precision leak valve. Purity of benzonitrile was verified using a UHV residual gas analyzer (Stanford Research Systems RGA300) before the start of dosing experiments. For metal atom chain growth experiments, indium was evaporated onto the sample surface using an Omicron EFM3 evaporator in a separate UHV chamber. Sample was positioned within the indium beam for a period of 10 min once a beam current of 100

Received: March 18, 2012
Published: August 22, 2012

ACS Publications © 2012 American Chemical Society

dx.doi.org/10.1021/ja3026399 | J. Am. Chem. Soc. 2012, 134, 15312−15317

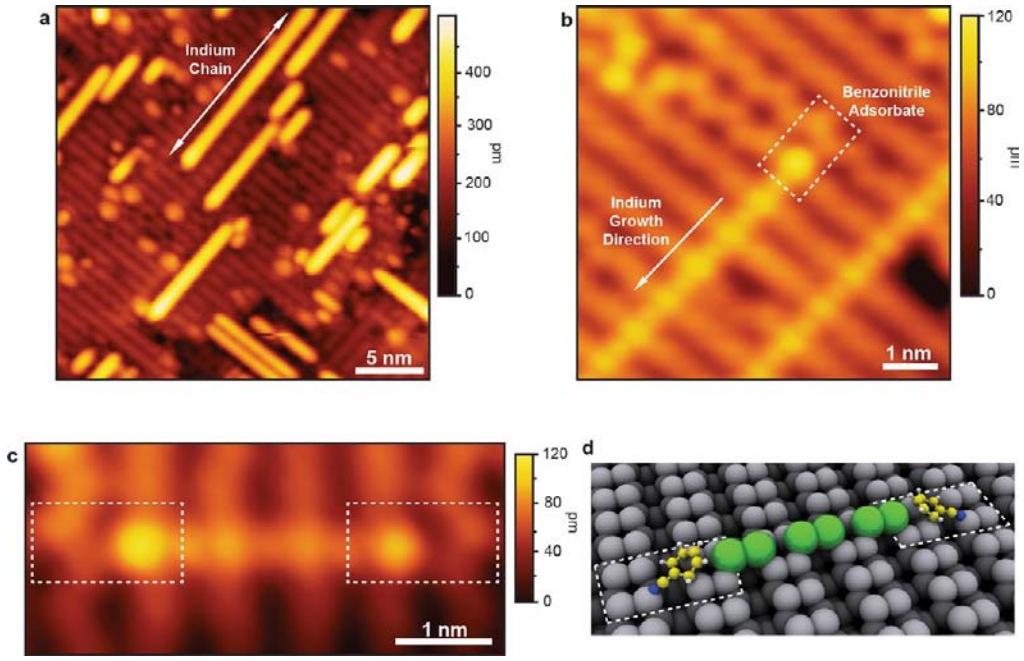

Figure 1. STM topographs showing individual chemisorbed benzonitrile molecules forming nucleation points for indium chain growth. (a) 25 × 25 nm^2 empty-state image (+1.2 V, 15 pA) showing indium chains perpendicular to the direction of the underlying dimer rows. (b) Filled-state (−1.6 V, 15 pA) STM image of an indium chain on the surface originating from an adsorbed benzonitrile molecule (dashed box). (c) Filled-state STM image of a single indium chain terminated at each end by benzonitrile molecules (−1.6 V, 15 pA). (d) Three-dimensional structural model corresponding to the experimental data in panel c.

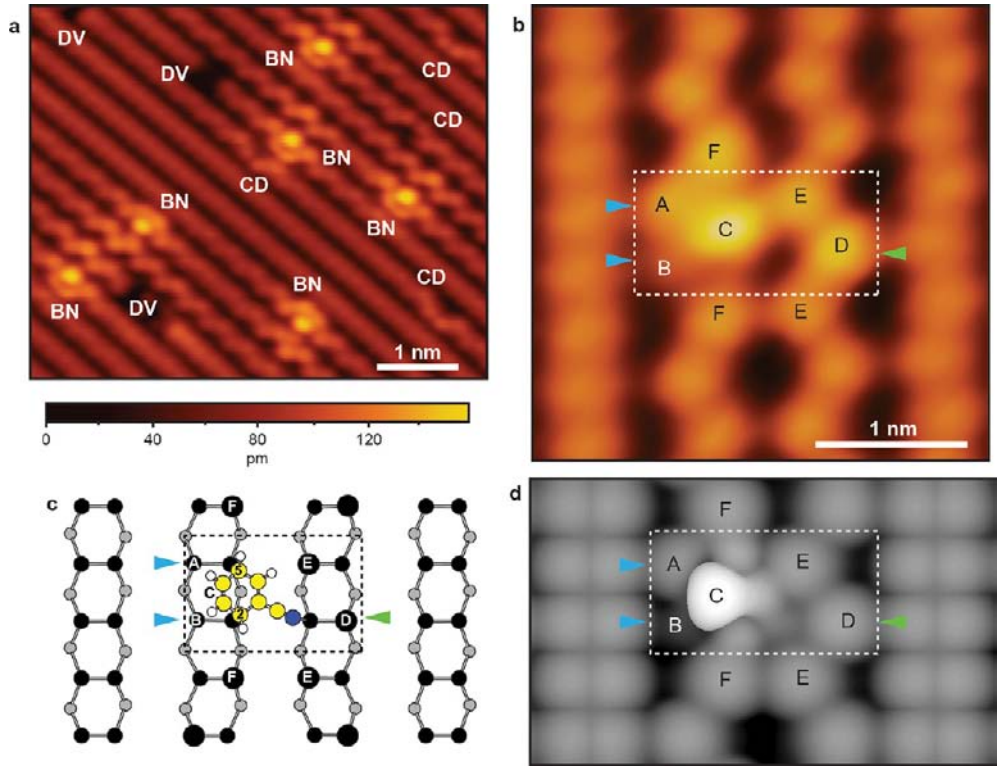

Figure 2. Benzonitrile adsorbates on the Si(001)2 × 1 surface at room temperature. (a) Filled-state STM image of the Si(001) surface, showing adsorbed benzonitrile molecules (BN), C defects (CD), and dimer vacancies (DV) (−1.6 V, 15 pA). (b) Filled-state STM image of an isolated adsorbate (−1.8 V, 15 pA), (c) structural model, and (d) simulated STM image (isosurface value 8.3 × 10^{-5} e/$Å^3$). Six key locations (A–F) are indicated in panels b–d. Locations A, B, and D indicate half-terminated Si dimer sites with dangling bonds (represented by arrowheads). Pair of blue arrowheads at sites A and B indicate the nucleation site for indium chain growth. Bright protrusion at site C is due to unsaturated π electrons between the end two C atoms of the ring. Adsorbate induces asymmetric pinning on the surface (sites E and F) evident by the zig-zagged appearance of the dimer rows to which the adsorbate is bonded.

dx.doi.org/10.1021/ja3026399 | J. Am. Chem. Soc. 2012, 134, 15312−15317

nA was established, before being transferred back to the main STM chamber without leaving UHV.

Ab initio, plane-augmented wave (PAW)[13,14] density functional theory calculations were performed using the VASP software,[15−18] with the exchange and correlation interactions treated in the generalized gradient approximation (GGA).[19−21] The silicon surface was represented using a slab containing four atomic layers of silicon terminated on the bottom by hydrogen atoms and separated from its periodic images in the plane-perpendicular direction by a vacuum gap of 20 Å. For the in-plane repeat we use a 6 × 5 supercell of 15 Si−Si dimers in three dimer rows. The top three silicon layers and all adsorbate atoms were fully relaxed until forces and energies were converged to below 1×10^{-2} eV/Å and 1×10^{-4} eV, respectively. Four special **k** points[22] were used to sample the irreducible symmetry element of the surface Brillouin zone. Simulated filled-state STM images[23] were calculated by integrating the local density of states within −1.5 eV of the Fermi level. To produce a realistic image of surface pinning, two different buckling configurations for each row were averaged whenever there was no appreciable energy shift between them. Nudged elastic band calculations were performed using the extended VASP transition state tool set.[24−26]

RESULTS AND DISCUSSION

In our experiments, Si(001) surfaces were first exposed to a small dose of benzonitrile and subsequently to a moderate fluence of indium atoms, as described above. This procedure results in a surface with randomly distributed, molecularly adsorbed benzonitrile molecules from which chains of indium atoms have grown; an unoccupied-state STM image of a typical surface produced by this procedure is shown in Figure 1a. All of the indium chains in this image extend from either a benzonitrile or a C-defect nucleation site, as was the case in all of our images of surfaces prepared according to this procedure. This observation is in agreement with previous reports of indium chain growth from C defects.[5,6] Figure 1b shows a slightly higher resolution image of the same surface that highlights a single indium chain. This image was acquired in occupied states where the structure of the nucleating benzonitrile adsorbate can be more clearly observed (dashed box). Figure 1c shows a similar image of an indium chain that is terminated at both ends by benzonitrile adsorbates.

Observation of indium chain nucleation at benzonitrile adsorbate sites suggests a similarity in the physical and electronic structures between this feature and the C defect. We investigated this similarity by imaging the benzonitrile-dosed surface prior to indium deposition and comparing these images with DFT calculations. The STM image in Figure 2a shows a 5.6 nm × 5.0 nm area of this surface where six benzonitrile adsorbates (BN), four C defects (CD), and three dimer vacancy defects (DV) can be seen. Benzonitrile adsorbates are all of identical appearance in this and the remainder of our STM images. Furthermore, no spontaneous structural changes or diffusion of the benzonitrile adsorbates were observed when imaging this surface under typical STM imaging conditions (±1.6 V, 15 pA) for long periods (>6 h continuously). These observations show that only a single bonding configuration exists for this adsorbate on the Si(001) surface at room temperature and low coverage. They also demonstrate that the adsorbate is stable in the absence of external stimulation (e.g., using the STM tip as described below). We note that these observations are consistent with previous experimental observations[28] of benzonitrile on Si(001), where it was shown using electron and vibrational spectroscopy techniques that only a single adsorbate configuration was present for substrate temperatures between 180 and 450 K. Figure 2b shows an enlarged image of a single benzonitrile adsorbate. We will describe the atomic structure of this feature below but note here that its appearance in the STM images is due as much to its effect on the surrounding Si dimers as to the molecular orbitals of the adsorbate itself. This is a common trait of STM images of small organic molecules on semiconductor surfaces.[27]

The bonding configuration of this adsorbate was determined through a comparison of DFT total energy and simulated image calculations with the experimental data. Of a host of possible molecularly adsorbed configurations considered, the structure shown in Figure 2c is both the energetically preferred configuration and the structure that produces the simulated STM image that is most consistent with the experimental images. This structure and its measured and simulated STM appearance are shown in Figure 2b−d with key elements correlated using labels A−F. Benzonitrile is found to bridge across the trough between two dimer rows, attaching with the phenyl ring to one dimer row and with the nitrile group to the other. Two carbon atoms of the ring (labeled 2 and 5 in Figure 2c) form covalent bonds with two adjacent dimers on the first row, which breaks the resonant π system in the ring. This produces a brightly imaging C═C double bond (labeled C) and two dangling bonds (A and B) at the unreacted silicon dimer ends. On the second row, the nitrile group forms a dative bond with a down-buckled Si atom, which creates a third dangling bond at the site labeled D. Static silicon dimer pinning is evident next to the adsorbate along the two dimer rows, with the phase of the free dimers being preserved on the nitrile side (E), and broken on the phenyl side (F) of the adsorbate. We note that three previous studies[28−30] have investigated benzonitrile adsorption configurations on Si(001). These expansive studies considered a wide range of individual structures falling into several classes including dative bonded, grafting via one or both of the π bonds of the nitrile or phenyl groups, and dissociative adsorption. However, none of these works considered the possibility that benzonitrile might bond across the trough between neighboring dimer rows. Herein lies one of the great strengths of STM for determination of adsorbate structural configurations, since the images shown in Figure 2a and 2b unequivocally demonstrate that the adsorbate is bonded across the trough. This in turn motived our exploration of trough-bridging structures in our DFT calculations, leading to the structural assignment discussed above (Figure 2c).

In terms of its chemical reactivity and ability to nucleate indium chain growth, the analogy between the benzonitrile adsorbate and the C defect is created by the two adjacent dangling bonds, A and B in Figure 2c. C defects are known to arise from fragmentation of water molecules into H and OH on two adjacent dimers of the surface.[11,12] Crucially, H and OH half-terminate two adjacent dimers in the C defect exactly as the phenyl ring does for benzonitrile, creating the two dangling bonds that are required for indium chain nucleation. This is illustrated for benzonitrile in Figure 3: the adsorbate is located on the right-hand side of the experimental image (rectangular box in Figure 3a) and retains almost all of the imaging characteristics of a lone benzonitrile adsorbate. Extending from the molecule toward the left-hand side is a bright line, which corresponds to four indium atoms bridging between three dimer rows. The simulated STM appearance and atomic structure of this configuration are shown in Figure 3b and 3c and are consistent with the experimental image.

dx.doi.org/10.1021/ja3026399 | J. Am. Chem. Soc. 2012, 134, 15312−15317

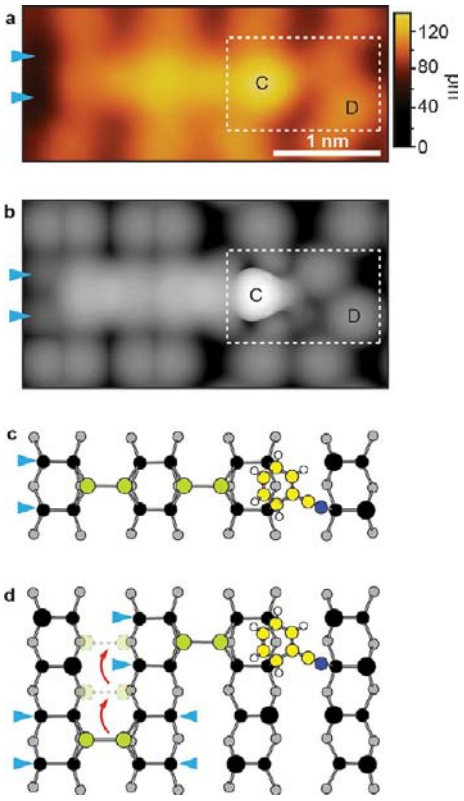

Figure 3. Indium chain extending from a benzonitrile adsorbate on Si(001) at room temperature. (a) Filled-state STM topograph of a benzonitrile molecule with an attached indium chain (−1.8 V, 15 pA). Arrowheads indicate the Si dangling bonds at the end of the chain. (b) Simulated STM image of an adsorbed benzonitrile molecule with four indium atoms calculated for the energetically preferred atomic configuration as shown in panel c. (c) Structural model for the energetically preferred arrangement of benzonitrile and four indium atoms. (d) Structure model of a precursor configuration to panel c showing a migrating indium atom pair in position to extend the existing benzonitrile−indium chain.

The structure of the indium atom chains is such that pairs of indium atoms bridge between the dimer rows.[5,6] Indium is a trivalent element, and thus, a pair of indium atoms is tetravalent, with two valencies at each end. These divalent ends provide a natural link with four Si atoms at the ends of two Si−Si dimers in adjacent rows, as shown in the bottom left of Figure 3d. As indicated by arrowheads in this figure, an isolated indium pair creates four half-terminated dimers and thus four dangling bonds, while the indium-pair/benzonitrile unit in the top right of the figure creates only two. Global reduction of the number of these dangling bonds is the basic principle behind the self-assembly of indium atoms into chains on Si(001): aligning the isolated indium pair with the indium-pair/benzonitrile unit (Figure 3c) reduces the number of dangling bonds from six to two.

The same stabilization is gained when pairs of indium atoms align with the pair of Si dangling bonds formed by either a benzonitrile adsorbate (locations A and B in Figure 2c) or a C defect. Density functional theory calculations confirm the salient aspects of this model. A pair of indium atoms is approximately 0.2 eV more stable than two separated indium adatoms. The alignment of an indium pair with another indium pair, a C defect, or a benzonitrile adsorbate leads to additional stabilizations of 0.3, 0.5, or 0.4 eV, respectively (see also refs 5−7). These energies confirm the qualitative model proposed above. In addition, we calculated the activation energies for indium diffusion. Noting that indium pairs move atom by atom,[7] we find the net barrier for diffusion of an isolated indium pair is 0.8 eV, while the barriers associated with shifting an indium pair into and out of alignment with a benzonitrile adsorbate are 0.8 and 1.0 eV, respectively. Our computational results thus both support and provide an explanation of the mechanism for indium-atom chain growth nucleated by benzonitrile adsorbates.

We observed this growth mechanism from image sequences involving diffusion of indium atoms between nearby competing benzonitrile adsorbates. Figure 4a shows a two dimer long indium chain extending from a benzonitrile adsorbate (BN1) with a neighboring indium-free adsorbate (BN2). Figure 4c is a later image of the same area where we see the indium atoms from the chain in Figure 4a have transferred from adsorbate BN1 to adsorbate BN2. Transfer of the indium chain occurs during the imaging of Figure 4b, where we image the chain partly in both locations. We are able to observe this transition since an uncapped indium chain is unstable at room temperature with indium atoms free to detach and reattach from their unterminated ends, as described above. We note that chains capped at both ends, such as that shown in Figure 1c, are stable, and indium diffusion was not observed from capped chains in our experiments.

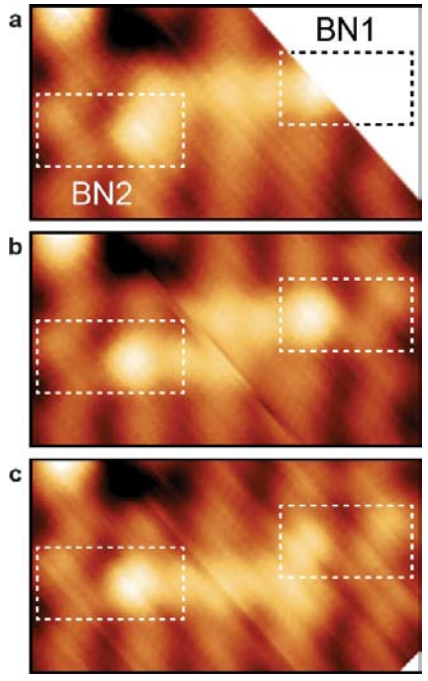

Figure 4. STM images (−1.6 V, 15 pA) showing the transfer of indium atoms between two competing benzonitrile nucleation sites at room temperature. (a) Two benzonitrile adsorbates on nearby Si dimer rows (see dashed boxes) offset by a single dimer. Indium chain is seen to originate from adsorbate BN1 (image at edge of scan region and partially clipped) and terminate adjacent to adsorbate BN2. (b) Image showing the chain originating at BN1 for part of the scan and shifting to the other benzonitrile adsorbate (BN2) for the remainder (note that the image has been rotated so that the slow and fast scan directions are rotated by 45° with respect to the figure axes). (c) Indium chain now originates from adsorbate BN2 and terminates adjacent to adsorbate BN1.

dx.doi.org/10.1021/ja3026399 | J. Am. Chem. Soc. 2012, 134, 15312−15317

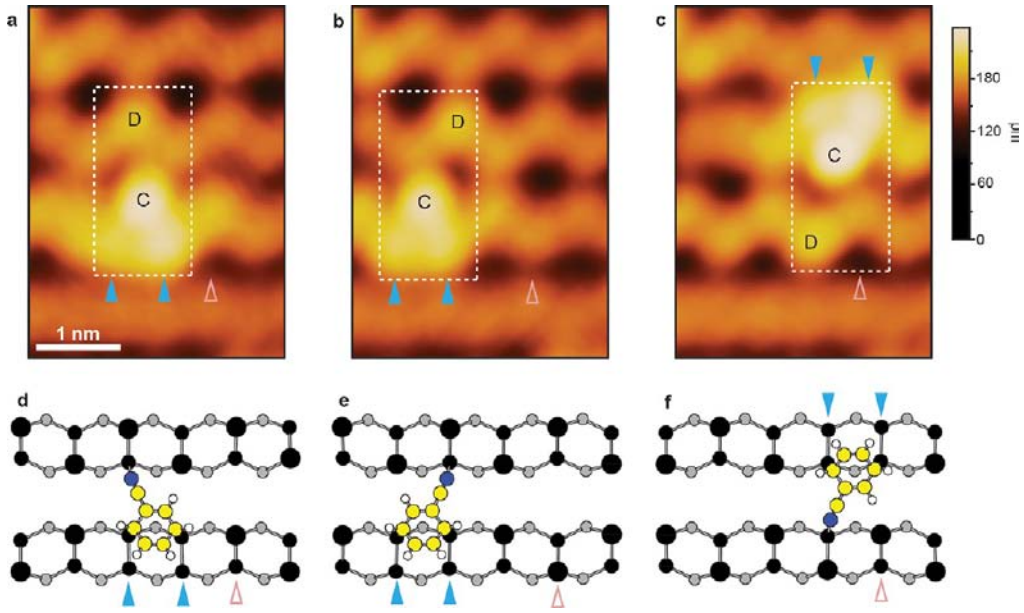

Figure 5. Manipulating an isolated benzonitrile adsorbate on Si(001) at room temperature through STM tip-induced excitations. (a) Benzonitrile adsorbate before manipulation (−1.6 V, 15 pA). White box indicates the adsorbate, while the open arrow points to the same surface atom in each of the panels. (b) Voltage pulse from −0.1 to −3.6 applied to the central protrusion (location C in Figure 2) induces the ring to shift positions along the dimer row without disruption to the Si−N bond. (c) Identical voltage pulse induces a rotation and lateral shift which involves breaking both of the original Si−C and Si−N bonds. (d−f) Structural models corresponding to images a−c.

The nucleating behavior of benzonitrile is not the only property that makes this adsorbate very interesting in the context of metal-atom chain growth. As mentioned, benzonitrile adsorbates on Si(001) exhibit the very useful property that they can be manipulated on the surface using a STM tip. By this we mean that individual benzonitrile adsorbates can be repositioned and reoriented on the surface in a nondestructive, reversible, and reproducible manner. We note that examples of such manipulations on semiconductor surfaces are rare, and the ability to do this on the technologically important Si(001) surface is of particular relevance for potential device applications.

Direct manipulation of individual adsorbates was achieved by positioning the STM tip above the adsorbate and increasing the tunnelling bias voltage while maintaining a constant tip−sample separation. Figure 5 shows an example of two such manipulations, producing a ∼50° rotation (Figure 5a and 5b) and a combined 180° rotation and 7.6 Å translation (Figure 5b and 5c), respectively. In these examples the STM tip was positioned directly above the brightly imaging ring portion of the adsorbate (location C) and the voltage was swept from 0 to −3.6 V (filled states) over a time of 300 ms. In 73% of 119 attempts the molecule was found to rotate or translate on the surface. A very different result was achieved when the same procedure was applied with the tip positioned above the nitrile end of the adsorbate (midpoint between positions E in Figure 2). In 16% of 67 attempts, sweeping the bias in this location resulted in complete desorption of the adsorbate from the surface. Our observations fit well with the interpretation of electron-stimulated manipulation and desorption as proposed for similar manipulations on the silicon surface.[31,32] The details of the physical mechanisms underlying these manipulations will be the subject of future studies. Of prime importance here is the proof-of-principle demonstration that individual benzonitrile adsorbates can be repositioned, reoriented, or desorbed from the Si(001) surface: this provides a path toward atomic-scale control of chain growth that does not require chemical passivation of the surface and thus provides a new type of control to complement existing lithographic approaches.

■ CONCLUSION

The results reported here show that benzonitrile molecules can nucleate the self-assembly of indium atoms into one-dimensional nanostructures on the Si(001) surface. These single-atom-wide structures grow from one side of a chemisorbed benzonitrile adsorbate, nucleating from a dangling bond pair created by the molecule. Importantly, the position and orientation of the chemisorbed molecule can be changed by STM manipulation, providing a means to control the position, direction, and length of the resultant structures. This is a fundamentally new approach to the controlled self-assembly of atoms on semiconductors, which can in principle be generalized to other atom/molecule/substrate combinations. In addition, further organic functionalization of the adsorbate can provide an opportunity to tailor the adsorbate with a view toward a more complex role, e.g., the capability to template inorganic chain growth in more than one direction or to act as an interface to other methods of forming nanostructures on silicon such as lithographic techniques[4] or self-directed organic chain growth.[27] However, perhaps the most exciting aspect of this technique lies in the implicit formation of a junction between a metal-atom chain and an organic molecule, a structure of central importance to the emerging field of single-molecule electronics.

■ AUTHOR INFORMATION

Corresponding Author

E-mail: Marian.Radny@newcastle.edu.au

Notes

The authors declare no competing financial interest.

■ ACKNOWLEDGMENTS

D.R.B. acknowledges the support of the Australian Government through the provision of a postgraduate scholarship. M.W.R. acknowledges support from the Polish Ministry of Science & Higher Education (Project no. N N202 169236). S.R.S acknowledges an Engineering and Physical Sciences Research Council (EPSRC) Career Acceleration Fellowship (EP/H003991/1). O.W. is supported by the Australian Research Council Centre of Excellence for Quantum Computation and Communication Technology (Project CE110001027). This project used computational resources provided by the Australian National Computational Infrastructure (NCI). We also thank K. Adam Rahnejat for rendering Figure 1d.

■ REFERENCES

(1) Wang, Q. H.; Hersam, M. C. *J. Am. Chem. Soc.* **2008**, *130*, 12896−12902.
(2) Lopinski, G. P.; Wayner, D. D.; Wolkow, R. A. *Nature* **2000**, *406*, 48−51.
(3) Hossain, M. Z.; Kato, H. S.; Kawai, M. *J. Am. Chem. Soc.* **2008**, *130*, 11518−11523.
(4) Lyding, J. W.; Shen, T. C.; Hubacek, J. S.; Tucker, J. R.; Abeln, G. C. *Appl. Phys. Lett.* **1994**, *64*, 2010−2012.
(5) Javorský, J.; Setvín, M.; Ošťádal, I.; Sobotík, P.; Kotrla, M. *Phys. Rev. B* **2009**, *79*, 165424−165432.
(6) Kocán, P.; Jurczyszyn, L.; Sobotík, P.; Ošťádal, I. *Phys. Rev. B* **2008**, *77*, 113301−113304.
(7) Radny, M. W.; Smith, P. V.; Jurczyszyn, L. *Phys. Rev. B* **2010**, *81*, 085424−085433.
(8) Yoon, H. S.; Ryu, M.-A.; Lyo, I.-W. *Surf. Sci.* **2003**, *547*, 210−218.
(9) Miki, K.; Bowler, D. R.; Owen, J. H. G.; Briggs, G. A. D.; Sakamoto, K. *Phys. Rev. B* **1999**, *59*, 14868−14871.
(10) Zhu, Y.; Zhou, W.; Wang, S.; Ji, T.; Hou, X.; Cai, Q. *J. Appl. Phys.* **2006**, *100*, 114312−114322.
(11) Hossain, M. Z.; Yamashita, Y.; Yoshinobu, J. *Phys. Rev. B* **2003**, *67*, 153307−153310.
(12) Yu, S.-Y.; Kim, H.; Koo, J.-Y. *Phys. Rev. Lett.* **2008**, *100*, 036107−036110.
(13) Blöchl, P. E. *Phys. Rev. B* **1994**, *50*, 17953−17979.
(14) Kresse, G.; Joubert, D. *Phys. Rev. B* **1999**, *59*, 1758−1775.
(15) Kresse, G.; Hafner, J. *Phys. Rev. B* **1993**, *47*, 558−561.
(16) Kresse, G.; Hafner, J. *Phys. Rev. B* **1993**, *49*, 14251−14269.
(17) Kresse, G.; Furthmüller, J. *Comput. Mater. Sci.* **1996**, *6*, 15−50.
(18) Kresse, G.; Furthmüller, J. *Phys. Rev. B* **1996**, *54*, 11169−11186.
(19) Perdew, J. P.; Wang, Y. *Phys. Rev. B* **1992**, *45*, 13244−13249.
(20) Perdew, J. P.; Chevary, J. A.; Vosko, S. H.; Jackson, K. A.; Perderson, M. R.; Singh, D. J.; Fiohais, C. *Phys. Rev. B* **1992**, *46*, 6671−6687.
(21) Perdew, J. P.; Chevary, J. A.; Vosko, S. H.; Jackson, K. A.; Perderson, M. R.; Singh, D. J.; Fiohais, C. *Phys. Rev B* **1993**, *48*, 4978.
(22) Monkhorst, H. J.; Pack, J. D. *Phys. Rev. B* **1976**, *13*, 5188−5192.
(23) Tersoff, J.; Hamann, D. R. *Theor. Phys. Rev. Lett.* **1983**, *50*, 1998−2001.
(24) Sheppard, D.; Terrell, R.; Henkelman, G. *J. Chem. Phys.* **2008**, *128*, 134106.
(25) Henkelman, G.; Uberuaga, B. P.; Jónsson, H. *J. Chem. Phys.* **2000**, *113*, 9901−9904.
(26) Henkelman, G.; Jónsson, H. *J. Chem. Phys.* **2000**, *113*, 9978−9985.
(27) Wolkow, R. A. *Annu. Rev. Phys. Chem.* **1999**, *50*, 413−441.
(28) Tao, F.; Wang, Z. H.; Xu, G. Q. *J. Phys. Chem. B* **2002**, *106*, 3557−3563.
(29) Qu, Y. −Q.; Han, K. −L. *J. Phys. Chem. B* **2004**, *108*, 8305−8310.
(30) Rangan, S.; Gallet, J. −J.; Bournel, F.; Kubsky, S.; Guen, K. L.; Dufour, G.; Rochet, F.; Sirotti, F.; Carniato, S.; Ilakovac, V. *Phys. Rev. B* **2005**, *71*, 165318−165329.
(31) Lastapis, M.; Martin, M.; Riedel, D.; Hellner, L.; Comtet, G.; Dujardin, G. *Science* **2005**, *308*, 1000−1003.
(32) Pan, T. L.; Sakulsermsuk, P. A.; Sloan, P. A.; Palmer, R. E. *J. Am. Chem. Soc.* **2011**, *133*, 11834−11836.